Hindawi Publishing Corporation
EURASIP Journal on Wireless Communications and Networking
Volume 2009, Article ID 739828, 11 pages
doi:10.1155/2009/739828

Research Article

Antenna Selection for MIMO Systems with Closely Spaced Antennas

Yang Yang,[1] Rick S. Blum,[1] and Sana Sfar[2]

[1] *Department of Electrical and Computer Engineering, Lehigh University, 19 Memorial Drive West, Bethlehem, PA 18015, USA*
[2] *CTO Office, InterDigital Communications, LLC, 781 Third Avenues, King of Prussia, PA 19406, USA*

Correspondence should be addressed to Yang Yang, yay204@lehigh.edu

Received 1 February 2009; Revised 18 May 2009; Accepted 28 June 2009

Recommended by Angel Lozano

Physical size limitations in user equipment may force multiple antennas to be spaced closely, and this generates a considerable amount of mutual coupling between antenna elements whose effect cannot be neglected. Thus, the design and deployment of antenna selection schemes appropriate for next generation wireless standards such as 3GPP long term evolution (LTE) and LTE advanced needs to take these practical implementation issues into account. In this paper, we consider multiple-input multipleoutput (MIMO) systems where antenna elements are placed side by side in a limited-size linear array, and we examine the performance of some typical antenna selection approaches in such systems and under various scenarios of antenna spacing and mutual coupling. These antenna selection schemes range from the conventional hard selection method where only part of the antennas are active, to some newly proposed methods where all the antennas are used, which are categorized as soft selection. For the cases we consider, our results indicate that, given the presence of mutual coupling, soft selection can always achieve superior performance as compared to hard selection, and the interelement spacing is closely related to the effectiveness of antenna selection. Our work further reveals that, when the effect of mutual coupling is concerned, it is still possible to achieve better spectral efficiency by placing a few more than necessary antenna elements in user equipment and applying an appropriate antenna selection approach than plainly implementing the conventional MIMO system without antenna selection.

1. Introduction

The multiple-input multiple-output (MIMO) architecture has been demonstrated to be an effective means to boost the capacity of wireless communication systems [1], and has evolved to become an inherent component of various wireless standards, including the next-generation cellular systems 3GPP long term evolution (LTE) and LTE advanced. For example, the use of a MIMO scheme was proposed in the LTE standard, with possibly up to four antennas at the mobile side, and four antennas at the cell site [2]. In MIMO systems, antenna arrays can be exploited in two different ways, which are [3]: diversity transmission and spatial multiplexing. However, in either case, one main problem involved in the implementation of MIMO systems is the increased complexity, and thus the cost. Even though the cost for additional antenna elements is minimal, the radio frequency (RF) elements required by each antenna, which perform the microwave/baseband frequency translation, analog-to-digital conversion, and so forth, are usually costly.

These complexity and cost concerns with MIMO have motivated the recent popularity of antenna selection (AS)—an attractive technique which can alleviate the hardware complexity, and at the same time capture most of the advantages of MIMO systems. In fact, for its low user equipment (UE) complexity, AS (transmit) is currently being considered as a baseline of the single-user transmit diversity techniques in the LTE uplink which is a MIMO single carrier frequency division multiple access (SC-FDMA) system [4]. Further, when it comes to the RF processing manner, AS can be categorized into two groups: (1) hard selection, where only part of the antennas are active and the selection is implemented in the RF domain by means of a set of switches (e.g., [5–7]); (2) soft selection, where all the antennas are active and a certain form of transformation is performed

in the RF domain upon the received signals across all the antennas (e.g., [8–10]).

A considerable amount of research efforts have been dedicated to the investigation of AS, and have solidly demonstrated the theoretical benefits of AS (see [3] for a tutorial treatment). However, previous works largely ignore the hardware implementation issues related to AS. For instance, the physical size of UE such as mobile terminals and mobile personal assistants, are usually small and invariable, and the space allocated for an antenna array is limited. Such limitation makes the close spacing between antenna elements a necessity, inevitably leading to mutual coupling [11], and correlated signals. These issues have caught the interest of some researchers, and the capacity of conventional MIMO systems (without AS) under the described limitations and circumstances was investigated, among others, in [12–17]. To give an example, the study in [12] shows that as the number of receive antenna elements increases in a fixed-length array, the system capacity firstly increases to saturate shortly after the mutual coupling reaches a certain level of severeness; and drops after that.

Form factors of UE limit the performance promised by MIMO systems, and can further affect the proper functionality of AS schemes. These practical implementation issues merit our attention when designing and deploying AS schemes for the 3GPP LTE and LTE advanced technologies. There exist some interesting works, such as [18, 19] which consider AS in size sensitive wireless devices to improve the system performance. But in general, results, conclusions, and ideas on the critical implementation aspects of AS in MIMO systems still remain fragmented. In this paper, through electromagnetic modeling of the antenna array and theoretical analysis, we propose a comprehensive study of the performance of AS, to seek more effective implementation of AS in size sensitive UE employing MIMO where both mutual coupling and spatial correlation have a strong impact. In this process, besides the hybrid selection [5–7], a conventional yet popular hard AS approach, we are particularly interested in examining the performance potential of some typical soft AS schemes, including the FFT-based selection [9] and the phase-shift-based selection [10], that are very appealing but seem not to have attracted much attention so far. At the meantime, we also intend to identify the operational regimes of these representative AS schemes in the compact antenna array MIMO system. For the cases we consider, we find that in the presence of mutual coupling, soft AS can always achieve superior performance as compared to hard AS. Moreover, effectiveness of these AS schemes is closely related to the interelement spacing. For example, hard AS works well only when the interelement spacing is no less than a half wavelength.

Additionally, another goal of our study is to address a simple yet very practical question which deals with the cost-performance tradeoff in implementation: as far as mutual coupling is concerned, can we achieve better spectral efficiency by placing a few more than necessary antenna elements in size sensitive UE and applying a certain adequate AS approach than plainly implementing the conventional MIMO system without AS? Further, if the answer is yes, how would we decide the number of antenna elements for placement and the AS method for deployment? Our work will provide answers to the above questions, and it turns out the solution is closely related to identifying the saturation point of the spectral efficiency.

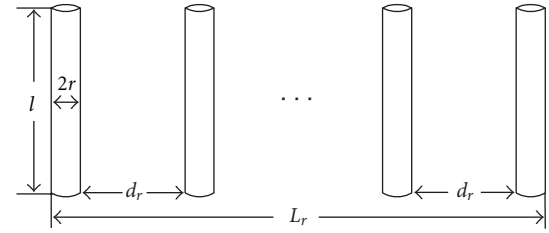

Figure 1: Dipole elements in a side-by-side configuration (receiver antenna array as an example).

This paper is organized as follows. In Section 2, we introduce the network model for the compact MIMO system and characterize the input-output relationship by taking into account the influence of mutual coupling. In Section 3, we describe the hard and soft AS schemes that will be used in our study, and also estimate their computational complexity. In Section 4, we present the simulation results. We discuss our main findings in Section 5, and finally conclude this paper in Section 6.

2. Network Model for Compact MIMO

We consider a MIMO system with M transmit and N receive antennas (M, $N > 1$). We assume antenna elements are placed in a side-by-side configuration along a fixed length at each terminal (transmitter and receiver), as shown in Figure 1. Other types of antenna configuration are also possible, for example, circular arrays [11]. But it is noted that, the side-by-side arrangement exhibits larger mutual coupling effects since the antennas are placed in the direction of maximum radiation [11, page 474]. Thus, the side-by-side configuration is more suitable to our study. We define L_t and L_r as the aperture lengths for transmitter and receiver sides, respectively. In particular, we are more interested in the case that L_r is fixed and small, which corresponds to the space limitation of the UE. We denote l as the dipole length, r as the dipole radius, and d_r (d_t) as the side-by-side distance between the adjacent dipoles at the receiver (transmitter) side. Thus, we have $d_r = L_r/(N-1)$ and $d_t = L_t/(M-1)$.

A simplified network model (as compared to [13, 14], e.g.) for transmitter and receiver sides is depicted in Figure 2. Figure 3 illustrates a direct conversion receiver that connects the output signals in Figure 2, where LNA denotes the low-noise amplifier, LO denotes the local oscillator, and ADC denotes the analog-to-digital converter. For the ease of the following analysis, we assume that in the circuit setup, all the antenna elements at the receiver side are grounded through the load impedance Z_{Li}, $i = 1, \ldots, N$ (cf. Figure 2), regardless of whether they will be selected or not. In fact, $Z_{L_i}, i = 1, \ldots, N$ constitute a simple matching circuit. Such matching circuit is necessary as it can enhance the efficiency of power

transfer from the generator to the load [20, Chapter 11]. We also assume that the input impedance of each LNA in Figure 3 which is located very close to the antenna element to amplify weak received signals, is high enough such that it has little measurable effect on the receive array's output voltages. This assumption is necessary to facilitate the analysis of the network model. However, it is also very reasonable because this ensures that the input of the amplifier will neither overload the source of the signal nor reduce the strength of the signal by a substantial amount [21].

Let us firstly consider the transmitter side, which can be regarded as a coupled M port network with M terminals. We define $\mathbf{i} = [i_1, \ldots, i_M]^T$ and $\mathbf{v}_t = [v_{t1}, \ldots, v_{tM}]^T$ as the vectors of terminal currents and voltages, respectively, and they are related through

$$\mathbf{v}_t = \mathbf{Z}_T \mathbf{i}, \tag{1}$$

where $\mathbf{Z}_T$ denotes the impedance matrix at the transmitter side. The (p,q)-th entry of $\mathbf{Z}_T(p,q)$, when $p \neq q$, denotes the mutual impedance between two antenna elements, and is given by [20, Chapter 21.2]:

$$\mathbf{Z}_T(p,q) = \frac{j\eta}{4\pi \sin^2(kl/2)} \int_{-l/2}^{l/2} F(z)\, dz, \tag{2}$$

where

$$F(z) = \left[\frac{e^{-jkR_1}}{R_1} + \frac{e^{-jkR_2}}{R_2} - 2\cos\left(\frac{kl}{2}\right) \cdot \frac{e^{-jkR_0}}{R_0} \right] \cdot \sin\left[k\left(\frac{l}{2} - |z| \right) \right]. \tag{3}$$

In the above expression, η denotes the characteristic impedance of the propagation medium, and can be calculated by $\eta = \sqrt{\mu/\epsilon}$, where μ and ϵ denote permittivity and permeability of the medium, respectively. Likewise, k denotes the propagation wavenumber of an electromagnetic wave propagating in a dielectric conducting medium, and can be computed through $k = \omega\sqrt{\mu\epsilon}$, where ω is the angular frequency. Finally R_0, R_1 and R_2 are defined as

$$R_0 = \sqrt{\frac{(p-q)^2 d_t^2}{(M-1)^2} + z^2},$$
$$R_1 = \sqrt{\frac{(p-q)^2 d_t^2}{(M-1)^2} + \left(z - \frac{l}{2}\right)^2}, \tag{4}$$
$$R_2 = \sqrt{\frac{(p-q)^2 d_t^2}{(M-1)^2} + \left(z + \frac{l}{2}\right)^2}.$$

When $p = q$, $\mathbf{Z}_T(p,q)$ is the self-impedance of a single antenna element, and can also be obtained from (2) by simply redefining R_0, R_1 and R_2 as follows:

$$R_0 = \sqrt{r^2 + z^2},$$
$$R_1 = \sqrt{r^2 + \left(z - \frac{l}{2}\right)^2}, \tag{5}$$
$$R_2 = \sqrt{r^2 + \left(z + \frac{l}{2}\right)^2}.$$

Thus, the self-impedance for an antenna element with $l = 0.5\lambda$ and $r = 0.001\lambda$ for example, is approximately

$$\mathbf{Z}_T(p,p) = 73.08 + 42.21j\,\Omega. \tag{6}$$

Further, let us consider an example that $M = 5$ antenna elements of such type are equally spaced over a linear array of length $L_t = 2\lambda$. The impedance matrix $\mathbf{Z}_T$ is given by

$$\mathbf{Z}_T = \begin{pmatrix} 73.08+42.21j & -12.52-29.91j & 4.01+17.73j & -1.89-12.30j & 1.08+9.36j \\ -12.52-29.91j & 73.08+42.21j & -12.52-29.91j & 4.01+17.73j & -1.89-12.30j \\ 4.01+17.73j & -12.52-29.91j & 73.08+42.21j & -12.52-29.91j & 4.01+17.73j \\ -1.89-12.30j & 4.01+17.73j & -12.52-29.91j & 73.08+42.21j & -12.52-29.91j \\ 1.08+9.36j & -1.89-12.30j & 4.01+17.73j & -12.52-29.91j & 73.08+42.21j \end{pmatrix}. \tag{7}$$

For $i = 1, \ldots, M$, the terminal voltage v_{ti} can be related to the source voltage x_i via the source impedance Z_{si} by $v_{ti} = x_i - Z_{si} i_i$. Define $\mathbf{Z}_S = \mathrm{diag}\{Z_{s1}, \ldots, Z_{sM}\}$, and $\mathbf{x} = [x_1, \ldots, x_M]$. Then, from Figure 2, we can obtain the following results: $\mathbf{v}_t = \mathbf{x} - \mathbf{Z}_S \mathbf{i}$ and $\mathbf{v}_t = \mathbf{Z}_T \mathbf{i}$. Therefore, the relationship between terminal voltages $\mathbf{v}_t$ and source voltages $\mathbf{x}$ can be written in matrix form as $\mathbf{v}_t = \mathbf{Z}_T(\mathbf{Z}_T + \mathbf{Z}_S)^{-1}\mathbf{x}$. Similar to [12], we choose $Z_{si} = \mathbf{Z}_T^*(i,i)$, which roughly corresponds to a conjugate match in the presence of mild coupling. In the case of uncoupling in the transmitter side, $\mathbf{Z}_T$ is diagonal, and its diagonal elements are all the same. Consequently, $\mathbf{Z}_T(\mathbf{Z}_T + \mathbf{Z}_S)^{-1}$ is also diagonal, and its diagonal element can be denoted as $\delta_T = \mathbf{Z}_T(1,1)/[\mathbf{Z}_T(1,1) + \mathbf{Z}_S(1,1)]$. To accommodate the special case of zero mutual coupling where $\mathbf{v}_t$ is equal to $\mathbf{x}$, in our model we modify the relationship between $\mathbf{v}_t$ and $\mathbf{x}$ into

$$\mathbf{v}_t = \mathbf{W}_T \mathbf{x}, \tag{8}$$

where $\mathbf{W}_T = \delta_T^{-1} \mathbf{Z}_T(\mathbf{Z}_T + \mathbf{Z}_S)^{-1}$.

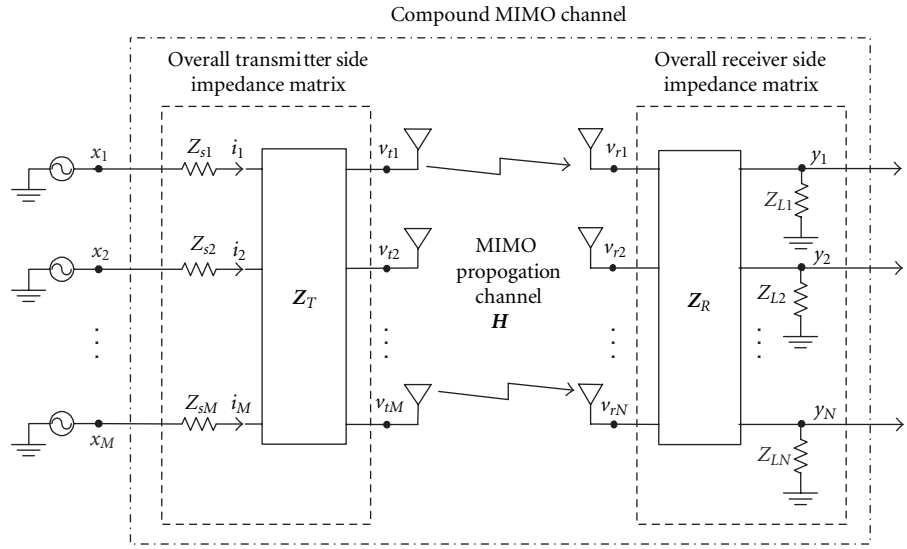

Figure 2: Network model for a (M, N) compact MIMO system.

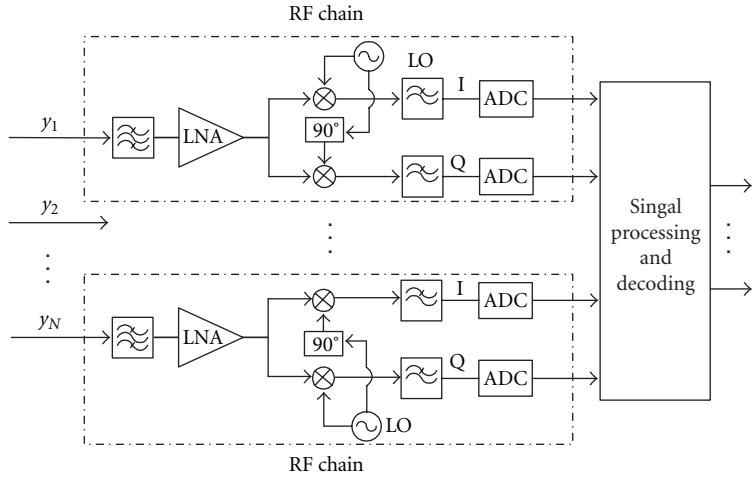

Figure 3: RF chains at the receiver side.

Denote $\mathbf{v}_r = [v_{r1}, \ldots, v_{rN}]$ as the vector of open circuited voltages induced across the receiver side antenna array, and $\mathbf{y} = [y_1, \ldots, y_N]$ as the voltage vector across the output of the receive array. Since we assumed high-input impedance of these LNAs, a similar network analysis can be carried out at the receiver side and will yield

$$\mathbf{y} = \mathbf{W}_R \mathbf{v}_r, \tag{9}$$

where $\mathbf{W}_R = \delta_R^{-1} \mathbf{Z}_L (\mathbf{Z}_R + \mathbf{Z}_L)^{-1}$. $\mathbf{Z}_R$ is the mutual impedance matrix at the receiver side, and $\mathbf{Z}_L$ is a diagonal matrix with its (i,i)th entry given by $\mathbf{Z}_L(i,i) = Z_{Li} = [\mathbf{Z}_R(i,i)]^*$, $i = 1, \ldots, N$. δ_R is given by $\delta_R = [\mathbf{Z}_R(1,1)]^* / \{\mathbf{Z}_R(1,1) + [\mathbf{Z}_R(1,1)]^*\}$. It is noted that the approximate conjugate match [12] is also assumed at the receiver side, so that the load impedance matrix $\mathbf{Z}_L$ is diagonal with its entry given by $\mathbf{Z}_R^*(i,i)$, for $i = 1, \ldots, N$.

In frequency-selective fading channels, the effectiveness of AS is considerably reduced [3], which in turn makes it difficult to observe the effect of mutual coupling. Therefore, we focus our attention solely on flat fading MIMO channels. The radiated signal $\mathbf{v}_t$ is related to the received signal $\mathbf{v}_r$ through

$$\mathbf{v}_r = \mathbf{H} \mathbf{v}_t, \tag{10}$$

where $\mathbf{H}$ is a $N \times M$ complex Gaussian matrix with correlated entries. To account for the spatial correlation effect and the Rayleigh fading, we adopt the *Kronecker model* [22, 23]. This model uses an assumption that the correlation matrix, obtained as $\boldsymbol{\Psi} = \mathrm{E}\{\mathrm{vec}(\mathbf{H})\ \mathrm{vec}(\mathbf{H})^H\}$ with $\mathrm{vec}(\mathbf{H})$ being the operator stacking the matrix $\mathbf{H}$ into a vector columnwise, can be written as a Kronecker product, that is, $\boldsymbol{\Psi} = \boldsymbol{\Psi}_R \otimes \boldsymbol{\Psi}_T$, where $\boldsymbol{\Psi}_R$ and $\boldsymbol{\Psi}_T$ are respectively, the receive and transmit correlation matrices, and $\otimes$ denotes the Kronecker product. This implies that the joint transmit and receive angle power spectrum can be written as a product of two independent

angle power spectrum at the transmitter and receiver. Thus, the correlated channel matrix $\mathbf{H}$ can be expressed as

$$\mathbf{H} = \mathbf{\Psi}_R^{1/2}\mathbf{H}_w\mathbf{\Psi}_T^{1/2}, \tag{11}$$

where $\mathbf{H}_w$ is a $N \times M$ matrix whose entries are independent identically distributed (i.i.d) circular symmetric complex Gaussian random variables with zero mean and unit variance. The (i, j)-th entry of $\mathbf{\Psi}_R$ or $\mathbf{\Psi}_T$ is given by $J_0(2\pi d_{ij}/\lambda)$ [24], where J_0 is the zeroth order Bessel function of the first kind, and d_{ij} denotes the distance between the i,j-th antenna elements.

Therefore, based on (8)–(11), the output signal vector $\mathbf{y}$ at the receiver can be expressed in terms of the input signal $\mathbf{x}$ at the transmitter through

$$\mathbf{y} = \mathbf{W}_R\mathbf{\Psi}_R^{1/2}\mathbf{H}_w\mathbf{\Psi}_T^{1/2}\mathbf{W}_T\mathbf{x} + \mathbf{n} = \mathcal{H}\mathbf{x} + \mathbf{n}, \tag{12}$$

where $\mathcal{H} = \mathbf{W}_R\mathbf{\Psi}_R^{1/2}\mathbf{H}_w\mathbf{\Psi}_T^{1/2}\mathbf{W}_T$ can be regarded as a *compound channel matrix* which takes into account both the Rayleigh fading in wireless channels and the mutual coupling effect at both transmitter and receiver sides, and $\mathbf{n}$ is the thermal noise. For simplicity, we assume uncorrelated noise at the receiving antenna element ports. For the case where correlated noise is considered, readers are referred to [16, 17].

3. Hard and Soft AS for Compact MIMO

We describe here some typical hard and soft AS schemes that we will investigate, assuming the compact antenna array MIMO system described in Section 2. For hard AS, we focus only on the hybrid selection method [5–7]. For soft AS, we study two typical schemes: the FFT-based selection [9] which embeds fast Fourier transform (FFT) operations in the RF chains, and the phase-shift-based selection [10] which uses variable phase shifters adapted to the channel coefficients in the RF chains. For simplicity, we only consider AS at the receiver side with n_R antennas being chosen out of the N available ones, and we focus on a spatial multiplexing transmission.

We assume that the propagation channel is flat fading and quasistatic, and is known at the receiver. We also assume that the power is uniformly allocated across all the M transmit antennas, that is, $\mathrm{E}\{\mathbf{x}\mathbf{x}^H\} = P_0\mathbf{I}_M/M$. We denote the noise power as σ_n^2, and the nominal signal-to-noise ratio (SNR) as $\rho = P_0/\sigma_n^2$. Then assuming some codes that approach the Shannon limit quite closely are used, the spectral efficiency (in bits/s/Hz) of this (M, N) full-complexity (FC) compact MIMO system without AS could be calculated through [1]

$$C_{\mathrm{FC}}(M,N) = \log_2\left\{\det\left[\mathbf{I}_M + \frac{\rho}{M}\mathcal{H}^H\mathcal{H}\right]\right\}. \tag{13}$$

It is worth noting that the length limits of transmit and receive arrays, L_t and L_r, enter into the compound channel matrix $\mathcal{H}$ in a very complicated way. It is thus difficult to find a close-form analytical relationship between $C_{\mathrm{FC}}(M, N)$ and L_t (L_r). Consequently, using Monte Carlo simulations to evaluate the performance of spectral efficiency becomes a necessity.

To avoid detailed system configurations and to make the performance comparison as general and as consistent as possible, we only use the spectral efficiency as the performance of interest. Moreover, all these AS schemes we study here are merely to optimize the spectral efficiency, not other metrics. Since each channel realization renders a spectral efficiency value, the ergodic spectral efficiency and the cumulative distribution function (CDF) of the spectral efficiency will be both meaningful. We will then consider them as performance measures for our study.

3.1. Hybrid Selection. This selection scheme belongs to the conventional hard selection, where n_R out of N receive antennas are chosen by means of a set of switches in the RF domain (e.g., [5–7]). Figure 4(a) illustrates the architecture of the hybrid selection at the receiver side. As all the antenna elements at the receiver side are presumed grounded through the load impedance Z_{Li}, $i = 1, \ldots, N$, the mutual coupling effect will be always present at the receiver side. However, this can facilitate the channel estimation and allow us to extract rows from $\mathcal{H}$ for subset selection. Otherwise, the mutual coupling effect will vary with respect to the selected antenna subsets. For convenience, we define $\mathbf{S}$ as the $n_R \times N$ selection matrix, which extracts n_R rows from $\mathcal{H}$ that are associated with the selected subset of antennas. We further define $\mathcal{S}$ as the collection of all possible selection matrices, whose cardinality is given by $|\mathcal{S}| = \binom{N}{n_R}$. Thus, the system with hybrid selection delivers a spectral efficiency of

$$C_{\mathrm{HS}} = \max_{\mathbf{S}\in\mathcal{S}} \log_2\left\{\det\left[\mathbf{I}_M + \frac{\rho}{M}(\mathbf{S}\mathcal{H})^H(\mathbf{S}\mathcal{H})\right]\right\}. \tag{14}$$

Optimal selection that leads to C_{HS} requires an exhaustive search over all $\binom{N}{n_R}$ subsets of $\mathcal{S}$, which is evident by (14). Note that

$$\det\left[\mathbf{I}_M + \frac{\rho}{M}(\mathbf{S}\mathcal{H})^H(\mathbf{S}\mathcal{H})\right] = \det\left[\mathbf{I}_{n_R} + \frac{\rho}{M}(\mathbf{S}\mathcal{H})(\mathbf{S}\mathcal{H})^H\right]. \tag{15}$$

Then, the matrix multiplication in (14) has a complexity of $O(n_R M \cdot \min(n_R, M))$. Calculating the matrix determinant in (14) requires a complexity of $O((\min(n_R, M))^3)$. Thus, we can conclude that optimal selection requires about $O(|\mathcal{S}| \cdot n_R M \cdot \min(n_R, M))$ complex additions/multiplications. This estimated complexity for optimal selection can be deemed as an upper bound of the complexity of any hybrid AS scheme, since there exist some suboptimal but reduced complexity algorithms, such as the incremental selection and the decremental selection algorithms in [7].

3.2. FFT-based Selection. As for this soft selection scheme (e.g., [9]), a N-point FFT transformation (phase-shift only) is performed in the RF domain firstly, as shown in Figure 4(b), where information across all the receive antennas will be utilized. After that, a hybrid-selection-like scheme is applied to extract n_R out of N information streams.

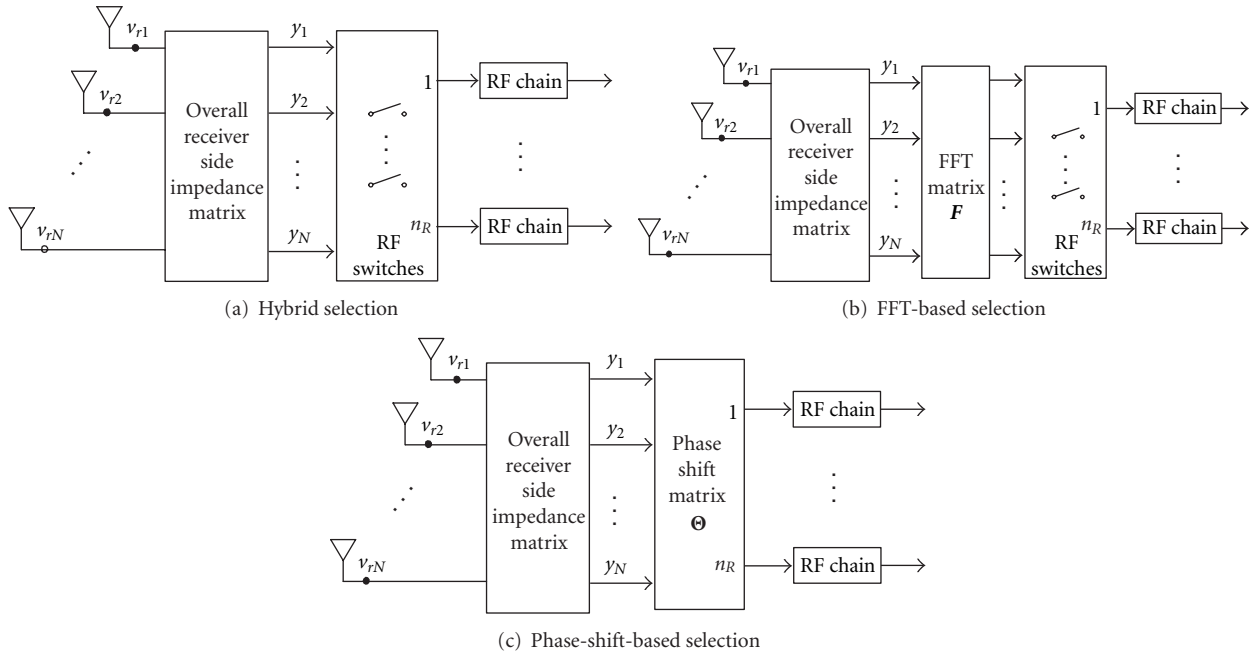

(a) Hybrid selection

(b) FFT-based selection

(c) Phase-shift-based selection

Figure 4: AS at the receiver side for spatial multiplexing transimssions.

We denote $\mathbf{F}$ as the $N \times N$ unitary FFT matrix with its (k,l) th entry given by:

$$\mathbf{F}(k,l) = \frac{1}{\sqrt{N}} \exp\left\{\frac{-j2\pi(k-1)(l-1)}{N}\right\}, \quad \forall k,l \in [1,N]. \tag{16}$$

Accordingly, this system delivers a spectral efficiency of

$$C_{\text{FFTS}} = \max_{\mathbf{S}\in\mathcal{S}} \log_2\left\{\det\left[\mathbf{I}_M + \frac{\rho}{M}(\mathbf{SF}\mathcal{H})^H(\mathbf{SF}\mathcal{H})\right]\right\}. \tag{17}$$

The only difference between (14) and (17) is the N-point FFT transformation. Such FFT transformation requires a computational complexity of $O(MN\log N)$. If we assume $N\log N \leq n_R \cdot \min(n_R, M)$, then the computational complexity of optimal selection that achieves C_{FFTS} can be estimated as $O(|\mathcal{S}| \cdot n_R M \cdot \min(n_R, M))$, which is the worst-case complexity.

3.3. Phase-Shift Based Selection. This is another type of soft selection scheme (e.g., [10]) that we consider throughout this study. Its architecture is illustrated in Figure 4(c). Let us denote $\boldsymbol{\Theta}$ as one $n_R \times N$ matrix whose elements are nonzero and restricted to be pure phase-shifters, that we will fully define in what follows. There exists some other work such as [25] that also considers the use of tunable phase shifters to increase the total capacity of MIMO systems. However, in Figure 4(c), the matrix $\boldsymbol{\Theta}$ that performs phase-shift implementation in the RF domain essentially serves as a N-to-n_R switch with n_R output streams. Additionally, unlike the FFT matrix, $\boldsymbol{\Theta}$ might not be unitary, and hence the resulting noise can be colored. Finally, this system's spectral efficiency can be calculated by [10]

$$C_{\text{PSS}} = \max_{\boldsymbol{\Theta}} \log_2\left\{\det\left[\mathbf{I}_M + \frac{\rho}{M}(\boldsymbol{\Theta}\mathcal{H})^H\left(\boldsymbol{\Theta}\boldsymbol{\Theta}^H\right)^{-1}(\boldsymbol{\Theta}\mathcal{H})\right]\right\}. \tag{18}$$

Let us define the singular value decomposition (SVD) of $\mathcal{H}$ as $\mathcal{H} = \mathbf{U}\boldsymbol{\Lambda}\mathbf{V}^H$, where $\mathbf{U}$ and $\mathbf{V}$ are $N \times N$, $M \times M$ unitary matrices representing the left and right singular vector spaces of $\mathcal{H}$, respectively; $\boldsymbol{\Lambda}$ is a nonnegative and diagonal matrix, consisting of all the singular values of $\mathcal{H}$. In particular, we denote $\lambda_{\mathcal{H},i}$ as the ith largest singular value of $\mathcal{H}$, and $\mathbf{u}_{\mathcal{H},i}$ as the left singular vector of $\mathcal{H}$ associated with $\lambda_{\mathcal{H},i}$. Thus one solution to the phase shift matrix $\boldsymbol{\Theta}$ can be expressed as [10, Theorem 2]:

$$\boldsymbol{\Theta} = \exp\left\{j \times \text{angle}\left\{\left[\mathbf{u}_{\mathcal{H},1}, \ldots, \mathbf{u}_{\mathcal{H},n_R}\right]^H\right\}\right\} \tag{19}$$

where angle$\{\cdot\}$ gives the phase angles, in radians, of a matrix with complex elements, exp$\{\cdot\}$ denotes the element-by-element exponential of a matrix.

The overall cost for calculating the SVD of $\mathcal{H}$ is around $O(MN \cdot \min(M,N))$ [26, Lecture 31]. Computing the matrix multiplication in (19) requires a complexity around the order of $O(MNn_R)$. The matrix determinant has an order of complexity of $O((\min(n_R, M))^3)$. Therefore, the phase-shift-based selection requires around $O(MN \cdot \max(n_R, M))$ complex additions/multiplications.

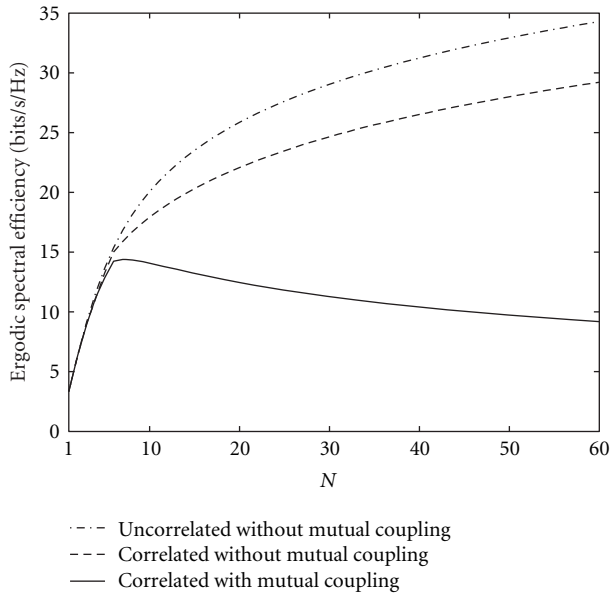

Figure 5: Ergodic spectral efficiency of a compact MIMO system ($M = 5$) with mutual coupling at both transmitter and receiver sides.

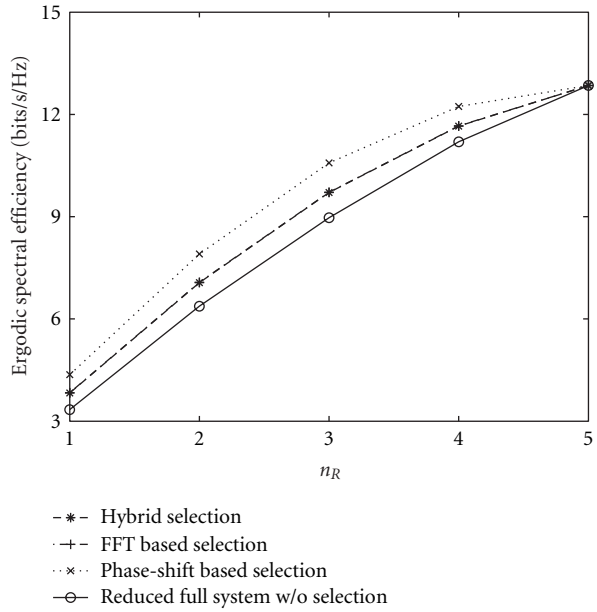

Figure 6: Ergodic spectral efficiency of a compact MIMO system with AS, where $M = 5$ and $N = 5$.

4. Simulations

Our simulations focus on the case when AS is implemented only on the receiver side, but mutual coupling and spatial correlation are accounted for at both terminals. However, in order to examine the mutual coupling effect on AS at the receiving antenna array, we further assume $M = 5$ equally-spaced antennas at the transmitter array, and the interelement spacing d_t is fixed at 10λ. This large spacing is chosen to make the mutual coupling effect negligible at the transmitting terminal. For the receiver terminal, we fix the array length L_r at 2λ. We choose $l = 0.5\lambda$ and $r = 0.001\lambda$ for all the dipole elements. Each component in the impedance matrices $\mathbf{Z}_T$ and $\mathbf{Z}_R$ is computed through (2) which analytically expresses the self and mutual impedance of dipole elements in a side-by-side configuration. Finally, we fix the nominal SNR at $\rho = 10$ dB.

As algorithm efficiency is not a focus in this paper, for both hybrid and FFT-based selection methods, we use the exhaustive search approach to find the best antenna subset. For the phase-shift-based selection, we compute the phase shift matrix $\mathbf{\Theta}$ through (19) given each $\mathcal{H}$. For each scenario of interest, we generate 5×10^4 random channel realizations, and study the performance in terms of the ergodic spectral efficiency and the CDF of the spectral efficiency.

4.1. Ergodic Spectral Efficiency of Compact MIMO. In Figure 5 we plot the ergodic spectral efficiency of a compact MIMO system for various N. The solid line in Figure 5 depicts the ergodic spectral efficiency when mutual coupling and spatial correlation is considered at both terminals. Also for the purpose of comparison, we include a dashed line which denotes the performance when only spatial correlation is considered at both sides, and a dash-dot line which corresponds to the case when only the simplest i.i.d Gaussian propagation channel is assumed in the system. It is clearly seen that mutual coupling in the compact MIMO system seriously decreases the system's spectral efficiency. Moreover, in accord with the observation in [12], our results also indicate that as the number of receive antenna elements increases, the spectral efficiency will firstly increase, but after reaching the maximum value (approximately around $N = 8$ in Figure 5), further increase in N would result in a decrease of the achieved spectral efficiency. It is also worth noting that when $N = 5$, the interelement spacing at the receiver side, d_r, is equal to $\lambda/2$, which probably is the most widely adopted interelement spacing in practice. Thus, results in Figure 5 basically indicate that, by adding a few more elements and squeezing the interelement spacing down from $\lambda/2$, it is possible to achieve some increase in the spectral efficiency, even in the presence of mutual coupling. But it is also observed that such increase is limited and relatively slow as compared to the spatial-correlated only case, and the spectral efficiency will saturate very shortly.

4.2. Ergodic Spectral Efficiency of Compact MIMO with AS. To study the performance of the ergodic spectral efficiency with regard to the number of selected antennas n_R for a compact MIMO system using AS, we consider three typical scenarios, namely, $N = 5$ in Figure 6, $N = 8$ in Figure 7, and $N = 12$ in Figure 8. In each figure, we plot the performance of the hybrid selection, FFT-based selection, and phase-shift-based selection. Additionally, we also depict in each figure the ergodic spectral efficiency of the reduced full-complexity (RFC) MIMO, denoted as $C_{\text{RFC}}(M, n_R)$, where only n_R receive antennas are distributed in the linear array and no AS is deployed. In Figure 6, it is observed that

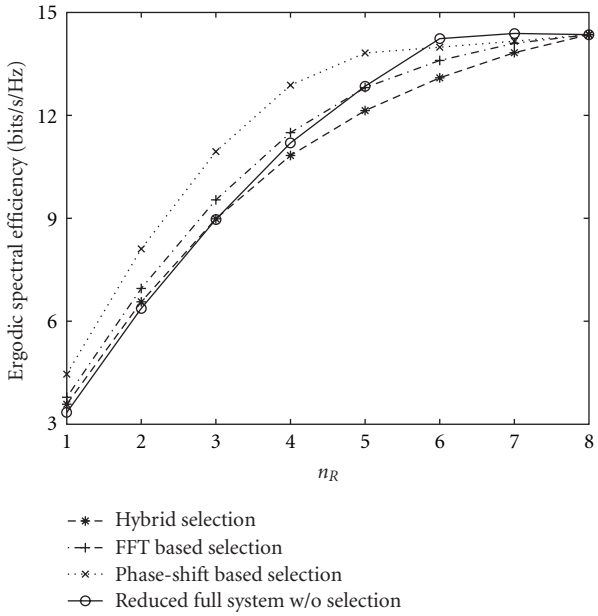

Figure 7: Ergodic spectral efficiency of a compact MIMO system with AS, where $M = 5$ and $N = 8$.

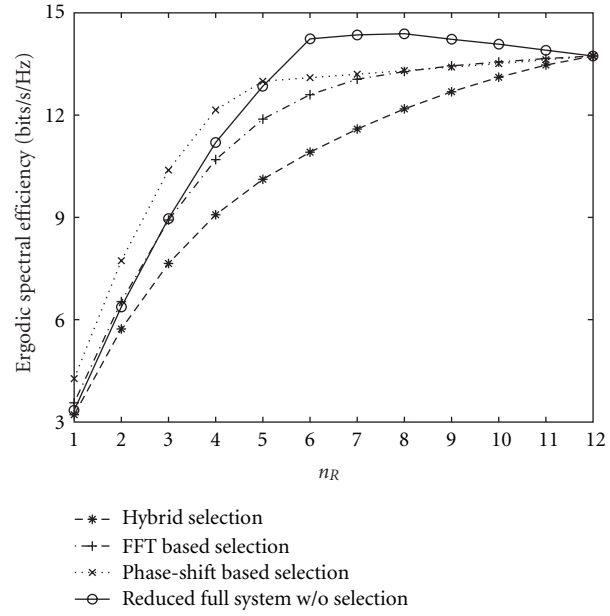

Figure 8: Ergodic spectral efficiency of a compact MIMO system with antenna selection, where $M = 5$ and $N = 12$.

$C_{\mathrm{FC}}(M = 5, N = 5) > C_{\mathrm{PSS}} > C_{\mathrm{FFTS}} = C_{\mathrm{HS}} > C_{\mathrm{RFC}}(M = 5, n_R)$, which in particular indicates the following:

(1) Soft AS always performs no worse than hard AS. The phase-shift-based selection performs strictly better than the FFT-based selection.

(2) With the same number of RF chains, the system with AS performs strictly better than the RFC system.

Interestingly, these conclusions that hold for this compact antenna array case are also generally true for MIMO systems without considering the mutual coupling effect (e.g., [10]). But a cross-reference to the results in Figure 5 can help understand this phenomenon. In Figure 5, it is shown that when N increases from 1 to 5, the ergodic spectral efficiency of the compact MIMO system behaves nearly the same as that of MIMO systems without considering the mutual coupling effect. Therefore, it appears natural that when AS is applied to the compact MIMO system with $N \leq 5$, similar conclusions can be obtained. It is also interesting that the FFT-based selection performs almost exactly the same as the hybrid selection.

Next we increase the number of placed antenna elements to $N = 8$, at which the compact MIMO system achieves the highest spectral efficiency (cf. Figure 5). We observe some different results in Figure 7, which are $C_{\mathrm{FC}}(M = 5, N = 8) > C_{\mathrm{PSS}} > C_{\mathrm{FFTS}} > C_{\mathrm{HS}}$. These results tell the following.

(1) Soft AS always outperforms hard AS. The phase-shift-based selection delivers the best performance among all these three AS schemes.

(2) The phase-shift-based selection performs better than the RFC system when $n_R \leq 5$. The FFT-based selection performs better than the RFC system when $n_R \leq 4$. The advantage of using the hybrid selection is very limited.

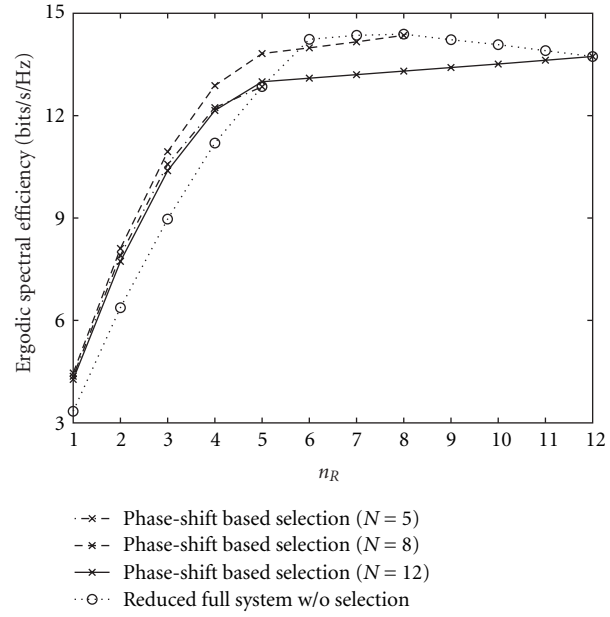

Figure 9: Ergodic spectral efficiency of a compact MIMO system with the phase-shift-based selection, where $M = 5$.

We further increase the number of antennas to $N = 12$. Now the mutual coupling effect becomes more severe, and different conclusions are demonstrated in Figure 8. It is observed that $C_{\mathrm{FC}}(M = 5, N = 12) > C_{\mathrm{PSS}} \geq C_{\mathrm{FFTS}} > C_{\mathrm{HS}}$, indicating the following.

(1) Soft AS performs strictly better than hard AS.

(2) The phase-shift-based selection performs better than the FFT-based selection when $n_R < 8$. After that, there is not much performance difference between them.

Also, similar to what we have observed in Figures 6 and 7, in terms of the ergodic spectral efficiency, none of the systems with AS outperforms the FC system with N receive antennas (and thus N RF chains). However, as for the RFC system with only n_R antennas (and thus n_R RF chains), in Figure 8 we observe the following.

(1) The RFC system always performs better than the hybrid selection. The hybrid selection seems futile in this case.

(2) The phase-shift-based selection performs better than the RFC system when $n_R < 5$. The benefit of the FFT-based selection is very limited, and it seems not worth implementing.

This indicates that due to the strong impact of mutual coupling in this compact MIMO system, only the phase-shift-based selection is still effective, but only for a limited range of numbers of the available RF chains. More specifically, when $n_R < 5$ it is best to use the phase-shift-based selection, otherwise the RFC system with n_R antennas when $5 \leq n_R < 8$. Further increase in the number of RF chains, however, will not lead to a corresponding increase in the spectral efficiency, as demonstrated in Figure 5.

For the purpose of comparison, we also plot the ergodic spectral efficiency of the phase-shift-based selection scheme in Figure 9, by extracting the corresponding curves from Figures 6–8. We find that by placing a few more antenna elements in the limited space so that the interelement spacing is less than $\lambda/2$, for example, $N = 8$ in Figure 9, the phase-shift-based selection approach can help boost the system spectral efficiency through selecting the best elements. In fact, the achieved performance is better than that of the conventional MIMO system without AS. This basically answers the question we posed in Section 1 that is related to the cost-performance tradeoff in implementation. However, further squeezing the interelement spacing will decrease the performance and bring no performance gain, as can be seen from the case of $N = 12$ in Figure 9.

4.3. Spectral Efficiency CDF of Compact MIMO with AS. In Figure 10, we investigate the CDF of the spectral efficiency for compact MIMO systems with $N = 8$. We consider the case of $n_R = 4$ in (Figure 10(a)) and $n_R = 6$ in (Figure 10(b)). We use dotted lines to denote the compact MIMO systems with AS, and dark solid lines for the FC compact MIMO systems (without AS). We also depict the spectral efficiency CDF-curves of the RFC systems of $N = 4$ and $N = 6$ in Figures 10(a) and 10(b), respectively in gray solid lines. As can be seen in Figure 10(a), soft AS schemes, that is, the phase-shift-based and FFT-based AS methods, perform pretty well as expected, but the hybrid selection performs even worse than the RFC system with $N = n_R = 4$ without AS. When we increase n_R to 6, as shown

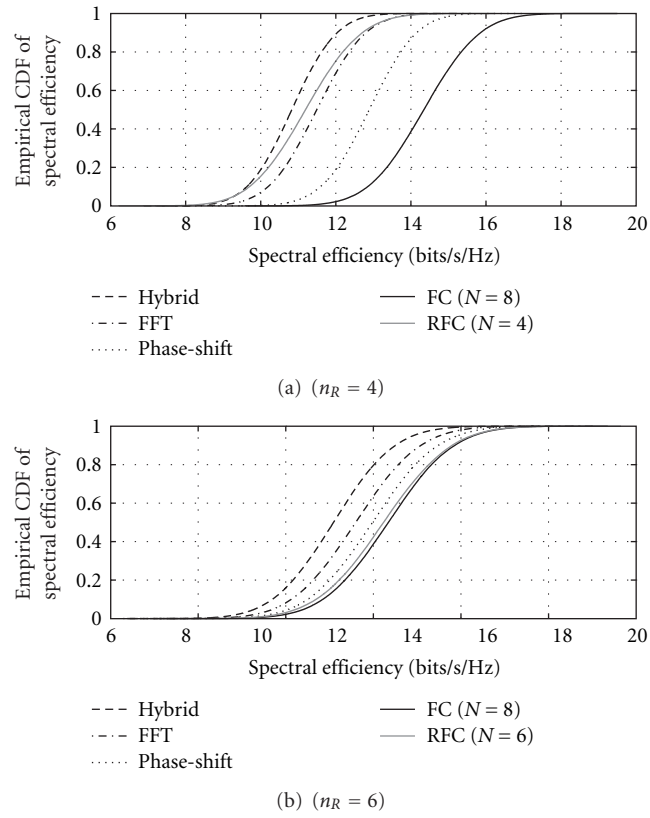

Figure 10: Empirical CDF of the spectral efficiency of a compact MIMO system with AS. $M = 5$ and $N = 8$.

in Figure 10(b), the performance difference between hard and soft AS schemes, or between the phase-shift-based and the FFT-based selection methods, is quite small. But none of these systems with various AS schemes outperform the RFC system of $N = n_R = 6$ without AS, which is consistent with what we have observed in Figure 7.

These results clearly indicate that when the mutual coupling effect becomes severe, the advantage of using AS can be greatly reduced, which however, is usually very pronounced in MIMO systems where only spatial correlation is considered at both terminals, as shown for example in Figure 11. On the other hand, it is also found that the spectral efficiency of a RFC system without AS, which is usually the lower bound spectral efficiency to that of MIMO systems with AS (as illustrated by an example of Figure 11), can become even superior to the counterpart when mutual coupling is taken into account (as shown in Figure 10 for instance). However, it should be noted that this phenomenon is closely related to the network model that we adopt in Section 2. In such model, we have assumed that all the antenna elements are grounded through the impedance $Z_{L_i}, i = 1, \ldots, N$, regardless of whether they will be selected or not. Thus, for MIMO systems with N receive elements and with a certain AS scheme, the mutual coupling impact at the receiver side comes from all these N elements, and is stronger than that of a RFC system with only n_R receive elements.

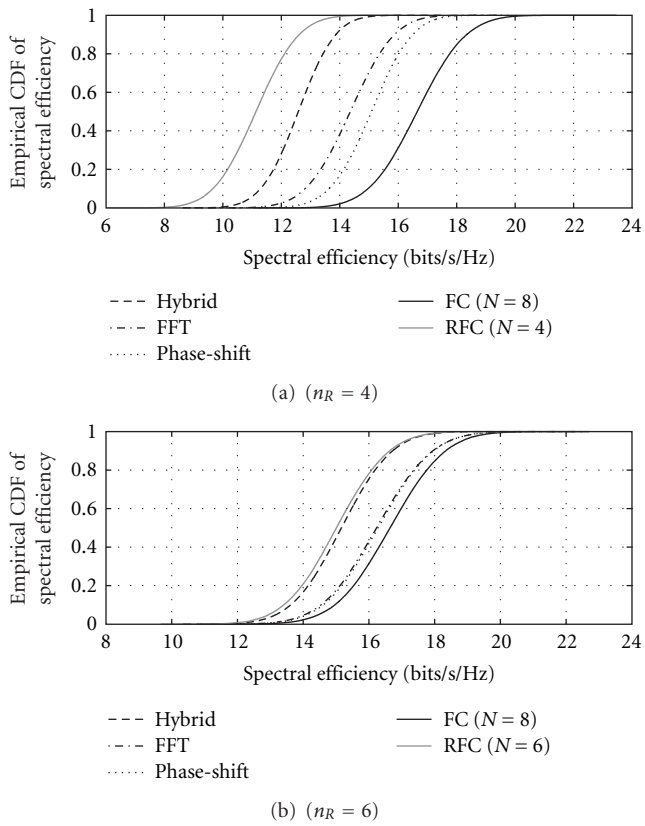

Figure 11: Empirical CDF of the spectral efficiency of a compact MIMO system with AS. $M = 5$, $N = 8$, and mutual coupling is not considered.

5. Discussions

In our study, we also test different scenarios by varying the length of linear array L_r, for example, we choose $L_r = 3\lambda$, 4λ, and so forth. For brevity, we leave out these simulation results here, but summarize our main findings as follows.

Suppose the ergodic spectral efficiency of a compact antenna array MIMO system saturates at N_{sat}. Our simulation results (e.g., Figure 5) indicate that

$$N_{\text{sat}} > \left\lfloor \frac{2L_r}{\lambda} + 1 \right\rfloor, \tag{20}$$

where $\lfloor \cdot \rfloor$ rounds the number inside to the nearest integer less than or equal to it. We also have $n_R < N$ for the sake of deploying AS. Our simulations reveal that the interelement spacing is closely related to the functionality of AS schemes. For the cases we study, the conclusion is the following:

(1) When $d_r \geq \lambda/2$, both soft and hard selection methods are effective, but the selection gains vary with respect to n_R. Particularly, the phase-shift-based selection delivers the best performance among these tested schemes. Performance of the FFT-based selection and the hybrid selection appears undistinguishable.

(2) When $d_r < \lambda/2$, there exist two situations:

(a) When $n_R \leq \lfloor 2L_r/\lambda + 1 \rfloor$, the selection gain of the phase-shift-based selection still appears pronounced, but tends to become smaller when n_R approaches $\lfloor 2L_r/\lambda + 1 \rfloor$. The advantage of using the FFT-based selection is quite limited. The hybrid selection seems rather futile.

(b) When $\lfloor 2L_r/\lambda + 1 \rfloor < n_R < N_{\text{sat}}$, neither soft nor hard selection seems effective. This suggests that AS might be unnecessary. Instead, we can simply use a RFC system with n_R RF chains by equally distributing the elements over the limited space.

It is noted that in all these cases we examine, soft AS always has a superior performance over hard selection. This is because soft selection tends to use all the information available, while hard selection loses some additional information by selecting only a subset of the antenna elements. Our simulation results also suggest that, if hard selection is to be used, it is necessary to maintain $d_r \geq \lambda/2$. Otherwise, the strong mutual coupling effect could render this approach useless. Further, if the best selection gain for system spectral efficiency is desired, one can place N_{sat} or so elements along the limited-length linear array, use $\lfloor 2L_r/\lambda + 1 \rfloor$ or less RF chains, and apply the phase-shift-based selection method. Therefore, it becomes crucial to identify the saturation point N_{sat}. This in turn requires the electromagnetic modeling of the antenna array that can take into account the mutual coupling effect.

6. Conclusion

In this paper, we proposed a study of some typical hard and soft AS methods for MIMO systems with closely spaced antennas. We assumed antenna elements are placed linearly in a side-by-side fashion, and we examined the mutual coupling effect through electromagnetic modeling of the antenna array and theoretical analysis. Our results indicate that, when the interelement spacing is larger or equal to one half wavelength, selection gains of these tested soft and hard AS schemes will be very pronounced. However, when the number of antennas to be placed becomes larger and the interelement spacing becomes smaller than a half wavelength, only the phase-shift-based selection remains effective and this is only true for a limited number of available RF chains. The same conclusions however, are not observed for the case of hard selection. Thus it seems necessary to maintain the interelement spacing no less than one half wavelength when the hard selection method is desired. On the other hand, if the best selection gain for system spectral efficiency is desired, one can employ a certain number of elements for which the compact MIMO system attains its maximum ergodic spectral efficiency, use $\lfloor 2L_r/\lambda + 1 \rfloor$ or less RF chains, and deploy the phase-shift-based selection method. This essentially indicates, if the cost-performance tradeoff in implementation is concerned, by placing a few more than necessary antenna elements so that the system spectral efficiency reaches saturation and deploying the phase-shift-based selection approach, we can achieve better

performance in terms of system spectral efficiency than the conventional MIMO system without AS. Overall, our study provides novel insight into the deployment of AS in future generation wireless systems, including the 3GPP LTE and LTE advanced technologies.

Acknowledgments

This material is based on research supported by the Air Force Research Laboratory under agreement FA9550-09-1-0576, by the National Science Foundation under Grant CCF-0829958, and by the U.S. Army Research Office under Grant W911NF-08-1-0449. The authors would like to thank Dr. Dmitry Chizhik and Dr. Dragan Samardzija of Bell Laboratories, Alcatel-Lucent for the helpful discussions on the modeling and implementation issues.

References

[1] G. J. Foschini and M. J. Gans, "On limits of wireless communications in a fading environment when using multiple antennas," *Wireless Personal Communications*, vol. 6, no. 3, pp. 311–335, 1998.

[2] Overview of 3GPP Release 8 V0.0.3, November 2008, http://www.3gpp.org/Release-8.

[3] A. F. Molisch and M. Z. Win, "MIMO systems with antenna selection," *IEEE Microwave Magazine*, vol. 5, no. 1, pp. 46–56, 2004.

[4] J. Kotecha, "LTE:MIMO Techniques in 3GPP-LTE," Freescale Semiconductor, June 2008.

[5] M. Z. Win and J. H. Winters, "Analysis of hybrid selection/maximal-ratio combining in Rayleigh fading," *IEEE Transactions on Communications*, vol. 47, no. 12, pp. 1773–1776, 1999.

[6] A. F. Molisch, M. Z. Win, and J. H. Winter, "Reduced-complexity transmit/receive-diversity systems," *IEEE Transactions on Signal Processing*, vol. 51, no. 11, pp. 2729–2738, 2003.

[7] A. Gorokhov, D. A. Gore, and A. J. Paulraj, "Receive antenna selection for MIMO spatial multiplexing: theory and algorithms," *IEEE Transactions on Signal Processing*, vol. 51, no. 11, pp. 2796–2807, 2003.

[8] L. Collin, O. Berder, P. Rostaing, and G. Burel, "Soft vs. hard antenna selection based on the minimum distance for MIMO systems," in *Proceedings of the 38th Asilomar Conference on Signals, Systems and Computers*, vol. 2, pp. 1369–1373, Grove, Calif, USA, November 2002.

[9] A. F. Molisch and X. Zhang, "FFT-based hybrid antenna selection schemes for spatially correlated MIMO channels," *IEEE Communications Letters*, vol. 8, no. 1, pp. 36–38, 2004.

[10] X. Zhang, A. F. Molisch, and S.-Y. Kung, "Variable-phase-shift-based RF-baseband codesign for MIMO antenna selection," *IEEE Transactions on Signal Processing*, vol. 53, no. 11, pp. 4091–4103, 2005.

[11] C. A. Balanis, *Antenna Theory: Analysis and Design*, John Wiley & Sons, New York, NY, USA, 3rd edition, 2005.

[12] R. Janaswamy, "Effect of element mutual coupling on the capacity of fixed length linear arrays," *IEEE Antennas and Wireless Propagation Letters*, vol. 1, pp. 157–160, 2002.

[13] C. Waldschmidt, S. Schulteis, and W. Wiesbeck, "Complete RF system model for analysis of compact MIMO arrays," *IEEE Transactions on Vehicular Technology*, vol. 53, no. 3, pp. 579–586, 2004.

[14] J. W. Wallace and M. A. Jensen, "Mutual coupling in MIMO wireless systems: a rigorous network theory analysis," *IEEE Transactions on Wireless Communications*, vol. 3, no. 4, pp. 1317–1325, 2004.

[15] A. A. Abouda and S. G. Häggman, "Effect of mutual coupling on capacity of MIMO wireless channels in high SNR scenario," *Progress in Electromagnetics Research*, vol. 65, pp. 27–40, 2006.

[16] M. J. Gans, "Channel capacity between antenna arrays—part I: sky noise dominates," *IEEE Transactions on Communications*, vol. 54, no. 9, pp. 1586–1592, 2006.

[17] M. J. Gans, "Channel capacity between antenna arrays—part II: amplifier noise dominates," *IEEE Transactions on Communications*, vol. 54, no. 11, pp. 1983–1992, 2006.

[18] Z. Xu, S. Sfar, and R. S. Blum, "On the importance of modeling the mutual coupling for antenna selection for closely-spaced arrays," in *Proceedings of IEEE Conference on Information Sciences and Systems (CISS '06)*, pp. 1351–1355, Princeton, NJ, USA, March 2006.

[19] D. Lu, D. K. C. So, and A. K. Brown, "Receive antenna selection scheme for V-BLAST with mutual coupling in correlated channels," in *Proceedings of IEEE International Symposium on Personal, Indoor and Mobile Radio Communications (PIMRC '08)*, pp. 1–5, Cannes, France, September 2008.

[20] S. J. Orfanidis, *Electromagnetic Waves and Antennas*, Rutgers University, Piscataway, NJ, USA, 2004.

[21] J. Hewes, "Impedance and reactance," The Electronics Club, February 2008, http://www.kpsec.freeuk.com/imped.htm.

[22] J. P. Kermoal, L. Schumacher, K. I. Pedersen, P. E. Mogensen, and F. Frederiksen, "A stochastic MIMO radio channel model with experimental validation," *IEEE Journal on Selected Areas in Communications*, vol. 20, no. 6, pp. 1211–1226, 2002.

[23] C. Oestges, B. Clerckx, D. Vanhoenacker-Janvier, and A. J. Paulraj, "Impact of fading correlations on MIMO communication systems in geometry-based statistical channel models," *IEEE Transactions on Wireless Communications*, vol. 4, no. 3, pp. 1112–1120, 2005.

[24] D.-S. Shiu, G. J. Foschini, M. J. Gans, and J. M. Kahn, "Fading correlation and its effect on the capacity of multielement antenna systems," *IEEE Transactions on Communications*, vol. 48, no. 3, pp. 502–513, 2000.

[25] Y. Nakaya, T. Toda, S. Hara, J.-I. Takada, and Y. Oishi, "Incorporation of RF-adaptive array antenna into MIMO receivers," in *Proceedings of IEEE Topical Conference on Wireless Communication Technology (WCT '03)*, pp. 297–298, Honolulu, Hawaii, USA, October 2003.

[26] L. N. Trefethen and D. Bau III, *Numerical Linear Algebra*, SIAM, Philadelphia, Pa, USA, 1997.